Review of Scientific Instruments ARTICLE pubs.aip.org/aip/rsi

Novel high-pressure/high-temperature reactor cell for *in situ* and *operando* x-ray absorption spectroscopy studies of heterogeneous catalysts at synchrotron facilities

Cite as: Rev. Sci. Instrum. 95, 055103 (2024); doi: 10.1063/5.0202557
Submitted: 5 February 2024 • Accepted: 15 April 2024 •
Published Online: 1 May 2024

Abdallah Nassereddine,[1,a] Alain Prat,[1,b] Samy Ould-Chikh,[2] Eric Lahera,[3] Olivier Proux,[3] William Delnet,[3] Anael Costes,[1] Isabelle Maurin,[1] Isabelle Kieffer,[3] Sophie Min,[3] Mauro Rovezzi,[3] Denis Testemale,[1] Jose Luis Cerrillo Olmo,[2] Jorge Gascon,[4] Jean-Louis Hazemann,[1] and Antonio Aguilar Tapia[5,a]

AFFILIATIONS

[1] Institut Néel, UPR 2940 CNRS - Université Grenoble Alpes, Grenoble F-38000, France
[2] KAUST Catalysis Center (KCC), King Abdullah University of Science and Technology (KAUST), Thuwal 23955, Saudi Arabia
[3] OSUG, UAR 832 CNRS - Université Grenoble Alpes, F-38041 Grenoble, France
[4] KAUST Catalysis Center (KCC), Advanced Catalytic Materials, King Abdullah University of Science and Technology (KAUST), Thuwal 23955, Saudi Arabia
[5] Institut de Chimie Moléculaire de Grenoble, UAR2607 CNRS- Université Grenoble Alpes, Grenoble F-38000, France

[a] **Authors to whom correspondence should be addressed:** abdallah.nassereddine@neel.cnrs.fr and antonio.aguilar@esrf.fr
[b] Deceased October 19, 2021.

ABSTRACT

This paper presents the development of a novel high-pressure/high-temperature reactor cell dedicated to the characterization of catalysts using synchrotron x-ray absorption spectroscopy under *operando* conditions. The design of the vitreous carbon reactor allows its use as a plug-flow reactor, monitoring catalyst samples in a powder form with a continuous gas flow at high-temperature (up to 1000 °C) and under high pressure (up to 1000 bar) conditions, depending on the gas environment. The high-pressure/high-temperature reactor cell incorporates an automated gas distribution system and offers the capability to operate in both transmission and fluorescence detection modes. The *operando* x-ray absorption spectroscopy results obtained on a bimetallic InCo catalyst during CO_2 hydrogenation reaction at 300 °C and 50 bar are presented, replicating the conditions of a conventional microreactor. The complete setup is available for users and permanently installed on the Collaborating Research Groups French Absorption spectroscopy beamline in Material and Environmental (CRG-FAME) sciences and French Absorption spectroscopy beamline in Material and Environmental sciences at ultra-high dilution (FAME-UHD) beamlines (BM30 and BM16) at the European Synchrotron Radiation Facility in Grenoble, France.

I. INTRODUCTION

Heterogeneous catalysts play a crucial role in various environmental and industrial applications, including the manufacturing of chemicals, pharmaceuticals, petroleum products, pollution control, and in the energy sector.[1] High-pressure gas phase reactions are encountered in various fields of chemistry. For instance, in the field of heterogeneous catalysis, different environmental and industrial reactions, such as CO_2 methanation, dimethyl ether synthesis, and methanol synthesis reactions, are thermodynamically favorable under high-pressure conditions.[2] Furthermore, catalytic processes at high pressure often lead to enhanced selectivity, minimizing the

formation of undesirable products.[3,4] In addition, the increase in pressure can influence reaction pathways and promote the formation of targeted products by suppressing secondary reactions.[2] In the case of CO_2 hydrogenation reaction, this improvement in selectivity is crucial, enabling the targeted production of chemicals, fuels, or other value-added materials from CO_2.[5] Moreover, in addition to enhancing kinetics and selectivity, high-pressure catalytic processes can also improve the stability and durability of catalysts.[6] The operation of metal catalysts under high pressure/temperature gaseous environments often leads to continuous modifications of their structural properties (crystalline structure, size, morphology, and composition), which dictate their catalytic performance. The fundamental understanding of the relationships between the structures and catalytic properties of catalysts at the molecular and atomic scale is crucial for identifying the nature of their active sites, understanding their activation and deactivation mechanisms, and ultimately, for designing more active catalysts.[7] A detailed understanding of reaction mechanisms in heterogeneous catalysis requires a precise description of the geometry and local environment of active sites, which are critical for the catalytic performance (conversion, selectivity, and stability). X-ray absorption spectroscopy (XAS), including x-ray absorption near-edge structure (XANES) and extended x-ray absorption fine structure (EXAFS), is currently one of the most well-established characterization techniques for studying heterogeneous catalysts.[8–15] Indeed, XAS provides information on the detailed local electronic (oxidation state) and geometric (nature, number, and distance of surrounding atoms) structure of the absorbing atom of the catalyst.

In the late 1970s, at the beginning of the synchrotron era, Lytle *et al.* in collaboration with the Exxon research group made important contributions to the development of *in situ* XAS cell technology.[16,17] The design of the cell enabled the regulation of gaseous or vaporous atmospheric conditions during XAS measurements. The cell material, composed of boron nitride, was chosen to minimize the x-ray absorption by the cell and ensure a sufficiently low level of absorption while housing the sample. This preliminary design allows for XAS experiments to be conducted on powdered and pelletized samples under conditions of up to 700 °C and 100 bar in transmission and fluorescence mode. Despite the significant range of applicable reaction conditions, the design has a drawback in that temperature regulation occurs on the furnace rather than in proximity to the catalyst sample. Furthermore, the cell large volume and associated external and internal mass transport limitations render it unsuitable for *operando* studies.[18] To avoid the issue of pore diffusion during sample measurements, a widely employed solution is the implementation of a highly versatile plug-flow cell design. This design uses a quartz glass capillary reactor that is heated by a hot air gas blower, thereby minimizing the impact of diffusion. The initial proposal of this idea was presented by Clausen *et al.*[19] and Sankar *et al.*[20] Subsequent advancements were made by Grunwaldt *et al.*,[18,21] which facilitated the integration of XAS with scattering techniques, such as x-ray diffraction (XRD), as well as optical spectroscopies, including UV–vis and Raman spectroscopy.[21–26] Despite the advancements achieved in *in situ*/*operando* studies, this design still poses some limitations, specifically the difficulty of conducting reactions at high pressures (>5 bar) and achieving uniform temperature distribution throughout the catalyst bed.[27–29]

In recent studies, there has been a focus on developing innovative designs to simultaneously characterize the catalyst and evaluate its catalytic performance. One notable approach by Bare *et al.* involved the development of a plug-flow reactor using beryllium tubes.[30] The enhanced design has demonstrated favorable potential for conducting XAS experiments at an elevated temperature (600 °C) and pressure (14 bar). In addition, this design has effectively mitigated mass transfer issues and facilitated precise replication of catalytic properties (conversion and selectivity) achieved under controlled laboratory conditions. The modifications made to this setup by Fingland *et al.* using borosilicate glass or polyimide tubes as reactor materials, both significantly less expensive and easier to work with, have further enabled the acquisition of high-quality data and accurate rate measurements.[31] However, the polyimide and borosilicate glass reactors possess a limited pressure rating, capable of accommodating only a few atmospheres. Moreover, polyimide tubing is constrained to temperatures below 400 °C and may deform even at lower temperatures. Indeed, at this temperature range, the authors reported the capillary deformation, resulting in its inclination with respect to the incident beam. As a result, the sample will no longer be exactly at the same position with respect to the beam, thus causing a signal modulation with temperature (the beam path in the sample is not constant) and so a decrease in the signal-to-noise ratio (even a complete loss of the signal if the sample is no more on the beam). This effect will directly impact the quality of XAS measurements. On the other hand, thin-walled borosilicate glass tubes are fragile and prone to cracking when compression fittings are used to create gas-tight seals, despite the use of PTFE ferrules. Three years later, the same research group proceeded to design a reactor by employing vitreous carbon as the material, aiming to increase its capability to withstand elevated temperatures and pressures for catalytic applications.[32] Thanks to its various properties, such as inertness, robustness, and high x-ray transmission, the use of this reactor revealed an enhanced capability to withstand high temperature (up to 600 °C) and high pressure (up to 25 bar). Rochet *et al.* reported the development of a plug-flow cell utilizing a "sandwich-like" reactor design at the SAMBA beamline at SOLEIL synchrotron to facilitate pressures up to 50 bar at the same temperature (600 °C) during the XAS experiment.[33] This XAS cell can be used with either powder samples or pellets under different gas atmospheres. However, this system can only be used for transmission mode XAS, which means that information about elements at lower concentration cannot be examined. Another issue is that the horizontal flow direction can result in the accumulation of unwanted liquid or waxy substances in the catalytic bed, potentially leading to blockages in the reactor. Very recently, Pandit *et al.* have developed a high-pressure reactor for the measurement of the structure and catalytic performance of copper-based catalysts during the hydrogenation of CO_2 to methanol.[34] Compared to the previous study conducted by Rochet *et al.*,[33] this new reactor shares a "sandwich design" similar to the one described in their study, but it offers certain advantages. It is capable of operating not only in transmission mode but also in fluorescence XAS mode and at high pressure of up to 50 bar. However, the operating temperature is limited to 450 °C. Furthermore, this reactor is applicable to other techniques, such as small-angle x-ray scattering (SAXS) and x-ray diffraction (XRD). Despite the inherent toxicity of beryllium and the associated handling challenges, the authors opted

to use it as the reactor material due to its robustness and adequate x-ray transmission capabilities. These advancements have played a crucial role in the progression of catalytic reaction studies and the understanding of material behavior within these reactions.[34–38] They have facilitated direct observation of the chemical and structural transformations taking place in materials during catalysis, particularly for high-pressure (up to 50 bar) reactions covering a wide temperature range (up to 600 °C). According to the various studies and developments described previously, achieving temperatures exceeding 800 °C and preventing temperature gradients on the catalyst bed poses a challenge. In order to address these challenges, our research group has recently made significant progress by developing a reaction cell using a glassy carbon reactor that can operate at elevated temperatures up to 1000 °C.[39] This innovative design ensures uniform heating of the sample region, thereby overcoming the mentioned difficulties. Various *in situ*/*operando* XAS studies of heterogeneous catalysts in a gaseous environment have further confirmed the significant progress achieved through the development of this setup.[40–45] However, this reaction cell is limited to catalytic reactions occurring under atmospheric pressure conditions.

Direct hydrogenation of CO_2 to methanol, using pure H_2 and CO_2 as reactants, represents a highly promising approach for CO_2 utilization, particularly when green hydrogen becomes accessible.[46–50] Furthermore, methanol has combined significant interest among the potential CO_2-derived products due to its applicability not only as an alternative fuel (e.g., in the production of dimethyl ether) but also as a convenient chemical feedstock (e.g., for the synthesis of formaldehyde and acetic acid).[51–55] In a study conducted by Bavykina *et al.*,[56] the authors prepared a novel and highly selective catalyst based on a combination of cobalt metal (Co) and oxidized indium (In). Separately, Co and oxidized In would produce methane and CO, respectively. However, the combination of these two elements showed a synergetic effect, leading to remarkable catalytic performances in terms of activity, selectivity, and stability during CO_2 hydrogenation reaction at 300 °C and 50 bar. More precisely, the InCo catalyst displayed significant selectivity toward methanol (69%) compared to CO (23%) and methane (8%), and it exhibited remarkable stability, maintaining around 19% CO_2 conversion rate over a duration of 100 h at 300 °C and 50 bar[56] In order to corroborate the catalytic results of the InCo catalysts obtained during this study, we were motivated to develop a high-pressure/high-temperature cell to monitor the catalyst structures under gaseous environment, high pressure, and temperature, using the XAS technique.

In the present work, we report a novel high-pressure/high-temperature reaction cell designed to work in both transmission and fluorescence detection modes (for the characterization of samples containing low element concentration). The objective is to integrate the high-temperature catalytic cell[39] into a high-pressure autoclave, which was also developed by our research team in 2005 for reproducing the experimental conditions associated with geological fluids using x-ray absorption and Raman spectroscopies.[57] For the catalytic application, we were inspired by the results reported by Bavykina *et al.*,[56] as an initial case study, to showcase the application of the novel high-pressure/temperature reactor setup in standard *operando* characterization within the field of heterogeneous catalysis. In this context, we conducted *operando* XAS measurements at the Co K-edge for an InCo catalyst during the CO_2 hydrogenation to methanol reaction at 300 °C and 50 bar. The high-pressure/high-temperature reaction cell is completed with an EcoCat-P portable mass spectrometer system provided by ESS. The mass spectrometer was positioned at the reactor outlet to enable the measurement of the composition of the gas products. This is equipped with two identical capillary inlets allowing the analysis of gas composition at both reactor outlets. The system has the capability to monitor up to 64 species in real time and offers detection levels down to ppb. This *in situ*/*operando* setup is available for users at the CRG-FAME and FAME-UHD (BM30 and BM16) beamlines at the European Synchrotron Radiation Facility (ESRF).

II. DESCRIPTION OF THE *IN SITU*/*OPERANDO* XAS CELL

The XAS reaction cell was designed to perform *in situ* and *operando* gas-phase experiments for heterogeneous catalysis applications. In our case, the samples, in the form of powder, necessitate gas flow, thermal treatment, and pressure regulation to reproduce the actual conditions implemented in a conventional laboratory microreactor. The optimization of our setup offers a safer handling of the device in comparison to systems using gas blower heaters. The heating part of our cell is isolated from the ambient so the body of the cell remains cold, which allows a safe handling and the possibility to approach detectors near the cell, which is important to improve the signal detection by fluorescence in diluted samples. Gas delivery is ensured by a fully automated and transportable gas distribution system. The gas distribution system includes a set of high-pressure mass flow controllers to precisely deliver the gas flow to the reaction cell. Notably, this setup is designed to be user-friendly, modular, and portable. Figure 1(a) shows the three-dimensional configuration of the novel high-pressure/temperature reactor, which draws inspiration from the previous designs outlined in our last high-temperature reaction cell development.[39] The reactor body is constructed entirely from X13 stainless steel material, chosen for its non-oxidizing properties and high strength, enabling it to withstand the specified pressures and temperatures. The glassy carbon tube is positioned within the heating elements. Concerning the sample heating, the previous design (high-temperature reactor cell) consists of placing the sample inside the reactor, which, in turn, is placed in a 30 mm molybdenum tube that allows heating of the sample through the surrounding resistive molybdenum metallic wires.[39] This configuration uses a pair of thermocouples: (i) one housed in a hole drilled in the molybdenum tube to control the temperature of the oven and (ii) another located inside the reactor in close proximity to the sample to monitor and control the sample temperature. Continuous external flow of ultra-pure He serves the dual object of protecting the carbon tube and molybdenum resistance against oxidation, particularly at high temperatures. The design of the current reactor heating system is based on the same design. However, this heating system includes just one thermocouple, inserted in a hole drilled inside the molybdenum tube for precise temperature control of the furnace (see more details in Sec. II B). Furthermore, the window materials of the new high-pressure/high-temperature reactor cell have changed compared to the old design. While the old design used Kapton windows (25 μm thick and 19 mm in diameter) to ensure high transmittance to x rays, the current design utilizes beryllium windows (Be SR200) with low absorption characteristics as well, but most importantly, excellent

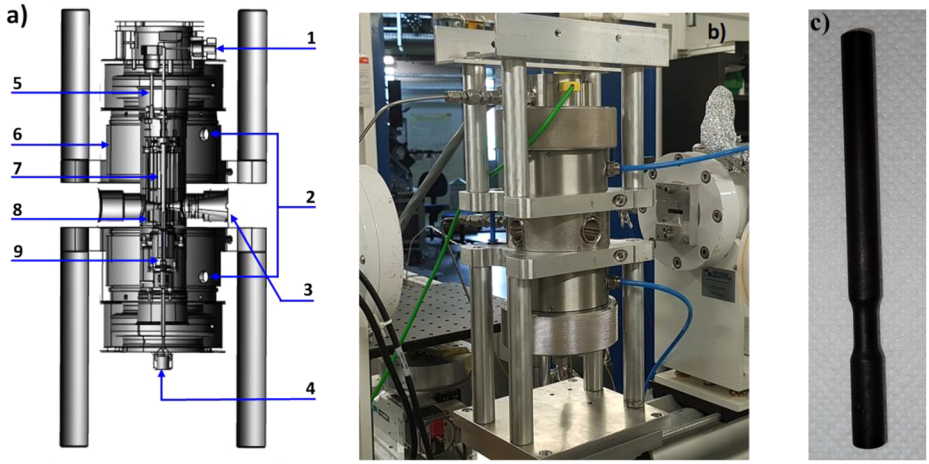

FIG. 1. (a) 3D layout of the reaction cell setup: (1) inlet of the gases to the cell, (2) plugs for cooling water circulation, (3) one of three windows, (4) gas outlet, (5) thermocouple to the heating system, (6) He inlet, (7) glassy carbon tube, (8) heating elements, and (9) region of the mixture of gas products and He; (b) real view of the fully assembled high-pressure/high-temperature cell in the SAMBA beamline at SOLEIL synchrotron ready for operation; and (c) glassy carbon reactor machined at 250 μm thickness wall at the window zone.

mechanical properties to ensure resistance of the cell during high-pressure operation (see more details in Sec. II C). Figure 1(b) shows a photograph of the fully assembled reaction cell at the SAMBA beamline in SOLEIL synchrotron. The image showcases one of the two transmission windows and the fluorescence window.

A. Fixed-bed reactor

Gases flow through the catalytic bed from the top to bottom through an innovative plug-flow reactor made of the glassy carbon tube [Fig. 1(c)] previously used in a high-temperature dedicated reaction cell developed in our research group.[39] The glassy carbon tubes were selected due to their distinct characteristics. They exhibit non-porosity and exceptional resistance to elevated temperatures, withstanding up to 3000 °C in an inert gas or vacuum environment and 600 °C in the presence of an oxidizing atmosphere.[58] The tube was machining in the window region, reducing its original wall thickness from 1 mm to 250 μm [Fig. 1(c)], thereby enabling effective transmission of the majority of the x-ray beam to the sample, with ~83% of the beam transmitted to the sample at the Co K-edge. This value demonstrates excellent suitability in comparison to a standard quartz capillary, which enables 92% and 84% transmission for wall thicknesses of 10 and 20 μm, respectively, at the same energy level.

The reactor is connected to the gas inlet and outlet tubes by bellows in the internal part of the cell, and the sealing is assured by using Viton joints. The design comprises a dedicated metallic rod used as a support for holding the quartz wool of the catalytic bed. The reaction cell can be fully dismounted to recover the glassy carbon tube. The glassy carbon reactor is filled by placing it on a support designed for this purpose (Fig. S1 in the supplementary material). The reactor is filled in the upper part with the quartz wool and the powder sample, and the powder is gently pressed. Then, the carbon tube containing the catalyst is placed inside the reaction cell and placed together in the sample stage of the beamline. At the end of the test, the cell is demounted, the sample is recovered, and the carbon tube is cleaned with ethanol. Thereafter, it is ready to be refilled with a new sample for a new experiment. The dismounting, cleaning, and remounting process takes around 20 min.

B. Heating system

The design of the current reactor heating system is based on the same design used for the development of our high-temperature reactor in 2018.[39] The heating element design was derived from the work of Tamura *et al.*[59] It involves positioning the reactor inside a 30 mm molybdenum tube [8 in Fig. 1(a)], which is heated to the desired experimental temperature using a resistive molybdenum metallic wire. In contrast to the previous system,[39] this heating system includes just one K-type thermocouple, inserted in a hole drilled inside the molybdenum tube to measure the temperature of our heating system. To prevent heat loss, all these components are enclosed in insulating ceramic elements. The cell design was based on a previously validated and certified catalytic reactor and autoclave development at the Néel Institute in Grenoble, and enables operation over a wide temperature range, from room temperature up to 1000 °C.[39,57] The cell is pressurized with ultra-pure He flow, which also prevents oxidation of the carbon tube and molybdenum resistance. The temperature control was achieved using a PID controller. After tuning the control system parameters, the reactor temperature could be smoothly ramped up from room temperature (RT) to the desired set point, employing a desired heating rate ranging from 2 to 20 °C/min, with minimal deviation during the ramping process and a stable control of the temperature at the set point with a deviation of ±0.66 °C.

C. Window materials and arrangement

Figure 2 shows a 3D drawing of the window configuration. The high-pressure/temperature cell was designed with three windows:

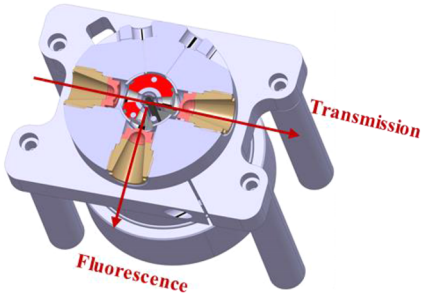

FIG. 2. 3D representation of the general geometry of Beryllium windows in the high-pressure/high-temperature reaction cell, illustrating two windows along the beam axis for spectrum collection in transmission mode and a third window positioned at a 90° angle to the beam for spectrum collection in fluorescence mode.

two positioned along the beam axis, one for entrance and the other for exit of the beam for measurements using transmission mode, and an additional one at 90° for working at fluorescence or inelastic scattering photons mode. One of the advantages of this cell is its ability to work in fluorescence mode, enabling the characterization of samples with very low concentrations of the elements of interest. Among the most versatile windows, suitable for the XAS technique, we use Beryllium as a material. Specifically, extruded Be SR200 was chosen for its favorable balance between excellent mechanical properties and low absorption characteristics. Window thickness is calculated as a function of working pressure. We use 0.8 mm Be windows for a working pressure of up to 300 bar, and then, we use 1 mm Be windows at a working pressure from 300 to 1000 bar. The high-pressure cell is cooled by the circulation of water to protect the windows from heating.

Because the sample is positioned at the center of the heating zone, the heating element was designed with three apertures with a diameter of 5 mm (22° wide aperture). These apertures allow the transmission of x-ray photons. This configuration additionally facilitates the vertical measurements of chemical inhomogeneity within the catalytic bed (~4 mm). This is achievable as the FAME beamline provides a beam spot of 200 × 100 μm^2 (HxV, FWHM), which can be moved along the reactor vertical axis. This is of particular importance when the reactor is operated under conditions of high reactant conversion. In such scenarios, the gaseous composition through the catalytic bed diverges substantially from that at the reactor inlet.

D. Pressure control and regulation

The reaction setup includes a completely automated high-pressure gas distribution system (Fig. S2 in the supplementary material) from Serv'Instrumentation to deliver up to four different gases. Each gas line is regulated by a high-pressure mass flow controller (in a range of 20–120 bar). Despite the limitation of our gas distribution system to introduce a maximum pressure of 120 bar, our high-pressure cell complies with European regulations, meeting the requirements of the Pressure Equipment Directive DESP 2014/68/UE, and has been certified to operate at pressures of up to 1000 bar, depending on the gas environment (see more details in the S3 section of the supplementary material).

The pressure in the cell increases as the reaction mixture flows through the glassy carbon reactor; simultaneously, helium flows through the cell body at the working pressure. The introduction of an inert gas, such as helium, allows for balancing the pressure throughout the system, followed by the extraction of the gaseous products formed at the reactor outlet. A pressure transmitter model Rosemount 2051, enables the equilibrium of the internal pressure between the glassy carbon tube and the body of the cell. The mixture of the products of the reaction and the He gas occurs immediately prior to the cell outlet [9 in Fig. 1(a)]. Precise pressure regulation is achieved at the reaction cell exit using the Brooks model SLA5820 pressure regulator. Furthermore, this regulator ensures release of the reaction mixture at atmospheric pressure. Finally, the gas distribution setup is provided with a liquid trap in order to protect the pressure regulator and the mass spectrometer.

The desired pressure set point can be manually adjusted through a control software, developed by Serv'Instrumentation, according to the specific requirements of the reaction conditions.

III. EXPERIMENTAL

A. Longitudinal temperature profile in the heating zone

The main drawback of our setup is the lack of the temperature measurement near the sample. To overcome this issue, a temperature profile test was conducted to assess the longitudinal temperature distribution within the 30 mm oven [8 in Fig. 1(a)]. The test was performed by flowing pure He through the cell and a second test by flowing the CO_2/H_2 reaction mixture, using different flow rates (10, 50, and 100 ml/min) in both cases. The test was performed maintaining a set point of 300 °C at atmospheric pressure. Figure 3 shows the temperature profile across the oven under varying He (A) and CO_2/H_2 reaction mixture (B) flow rates.

The shaded area in the figure (positioned at 12–17 mm along the oven) corresponds to the sample position. Remarkably, within the initial 5 mm of the oven, rapid heating of the gas occurs, in both cases [Figs. 3(a) and 3(b)], resulting in a homogeneous and stable temperature profile along the catalytic bed. This result is significant because it shows that the temperature remains constant and homogeneous regardless of the gas composition. The uniform temperature profile achieved within the reaction cell oven plays a crucial role in the study of catalysts under *operando* conditions. This feature stands as a distinct advantage compared to gas blower heaters,[30] in which temperature gradients may introduce imprecision in the measurement of the catalytic behavior. As previously discussed, gas blower heaters do not allow for homogeneous heating of the catalyst. In addition, the positioning of the gas blower with a capillary tube and the flow of the heating stream directly impact the sample temperature,[30] leading to a significant drawback when studying catalysts under *operando* conditions.

B. *Operando* XAS investigations of InCo catalyst during CO_2 hydrogenation reaction

The *operando* XAS measurements were performed at the SAMBA (spectroscopy applied to material based on absorption) beamline at the French National Synchrotron Facility (SOLEIL), Saint Aubin, France. The details of the beamline and its optical

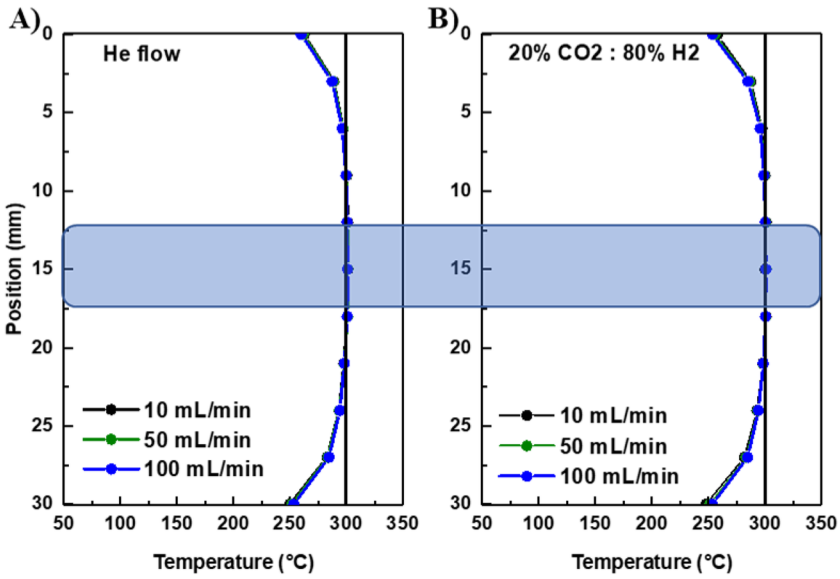

FIG. 3. Temperature profile along heating elements at set point = 300 °C with varied gas flows: (a) helium flow and (b) CO_2 hydrogenation reaction mixture 20% CO_2: 79% H_2: 1% Ar. The shaded area indicates the sample position (5 mm width).

devices have been described by Belin *et al.*[60] The beamline was equipped with a double-crystal Si 220 monochromator. The presence of two Pd-coated mirrors ensured the rejection of the harmonics to better than 0.1%, i.e., the intensity of the harmonics was less than 0.1% of the intensity of the fundamental x rays. The incident (I_0) and transmitted (I_1) intensities were measured by using ionization chambers. The measurements were carried out at the Co K-edge using fluorescence mode, and data acquisition employed a Canberra 35-element monolithic planar Ge pixel array detector.

The *operando* XAS characterization was made following the next protocol: a total amount of 100 mg InCo catalyst (sieved to a particle size range of 200–250 μm) was packed into the reactor to serve as the catalytic bed. The InCo catalyst was prepared following the same preparation method used by Bavykina *et al.*[56] Co K-edge XAS spectra were acquired under the helium atmosphere at room temperature to assess the initial state of the catalyst. Subsequently, the reactor was gradually heated up to 300 °C at a rate of 10 °C/min and then pressurized to 50 bars under He. XANES spectra were continuously recorded during the thermal treatment to monitor the change in the metal oxidation state. After thermal treatment under the He atmosphere, 50 ml/min of the reaction mixture comprising 20% CO_2, 79% H_2, and 1% Ar, diluted with 150 ml/min of He, was introduced. The reaction was stopped after 24 h, and then, EXAFS spectra were recorded to characterize the catalyst's final state. The XANES and EXAFS data were processed using the ATHENA program from the HORAE software package.[61]

To extract information about the proportion of the Cobalt species in the InCo catalyst, we applied linear combination fitting (LCF) analysis to the Co K-edge XANES spectra. The LCF method involves modeling the XAS spectra by least-squares fitting using a linear combination of known species to adjust an unknown spectra.[62] Indeed, this analysis method will determine the proportions of spectra (containing multiple species) for the selected reference compounds, which, when summed, yield the least-squares fit to the spectrum of an unknown sample.[63] The principle of this method is based on the additive nature of the absorption of each species in the sample. LCF analysis can be applied to both XANES and EXAFS spectra. The relative weights of the fractional components are allowed to vary from 0 to 1, and the resultant sum of all components is 1. In the present paper, LCF analysis was performed using Athena software and has been carried out in the normalized XAS spectra using the reference spectra from −30 to 80 eV.

To quantify the flow rate variation resulting from the reaction stoichiometry, a 1% argon tracer was incorporated into the reaction mixture (20% CO_2: 79% H_2: 1% Ar). Specifically, this involved utilizing mass spectrometry to monitor the stabilization of current intensities corresponding to m/z = 44 [$I(CO_2)i$] and m/z = 40 [I(Ar)i] for CO_2 and Ar gases, respectively, during the experiment. The quantification of reacted carbon dioxide was achieved by monitoring the current intensity corresponding to m/z = 44 [$I(CO_2)_f$] at the reactor outlet. Consequently, the conversion of carbon dioxide [$X(CO_2)$] during the reaction was calculated using the following equation:

$$X(CO_2)[\%] = \left[1 - \left(\frac{I(CO_2)_f}{I(CO_2)_i}\right)\left(\frac{I(Ar)_i}{I(Ar)_f}\right)\right] \times 100. \quad (1)$$

IV. RESULTS AND DISCUSSIONS

The objective of our study was to gain insights into the chemical state of cobalt in a methanol producer catalyst, specifically the InCo catalyst, during the induction phase of the reaction. To achieve this,

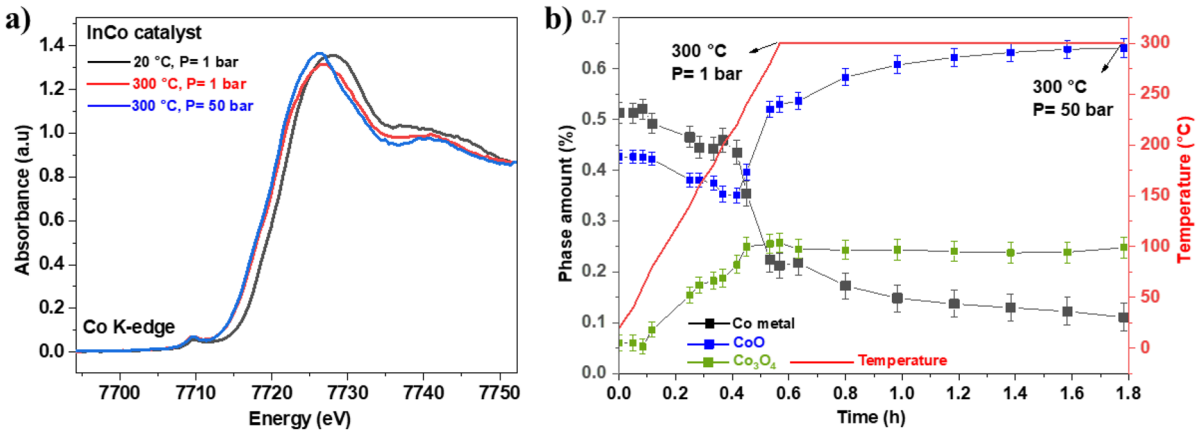

FIG. 4. Heating and pressurization of the InCo catalyst under helium. (a) Co K-edge XANES spectra of the InCo catalyst under He at the initial state (20 °C) after heating to 300 °C and then after pressurization to 50 bar at 300 °C. (b) Phase amount of Co species during the thermal treatment of the InCo catalyst under He up to 300 °C and pressurization up to 50 bars under He.

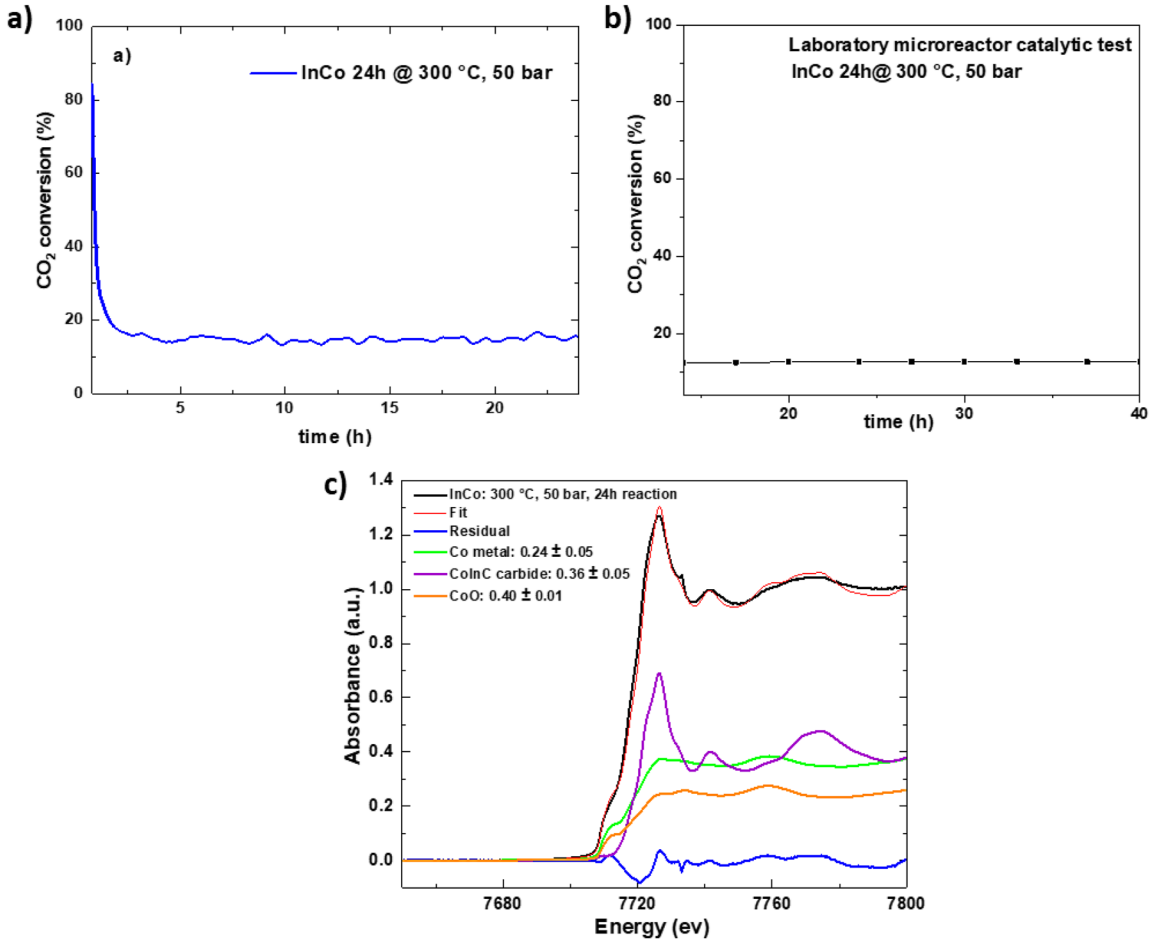

FIG. 5. (a) Evolution of the CO_2 conversion as a function of time at 300 °C and 50 bar in the high-pressure/high-temperature reaction cell. (b) Evolution of the CO_2 conversion as a function of time at 300 °C and 50 bar in the laboratory microreactor conditions. (c) Co K-edge XANES spectra at 300 °C and 50 bar and LCF of the XANES spectra of InCo catalysts after 24 h of CO_2 hydrogenation reaction (final state).

catalyst characterization was conducted under high-pressure reaction conditions at the SAMBA beamline in the synchrotron SOLEIL, under real conditions for the CO_2 hydrogenation reaction at 300 °C and 50 bar.

In the present study, the LCF analysis method was applied to determine the proportions of different cobalt phases based on the near-edge spectra region spanning from 7690 to 7790 eV, acquired during the thermal treatment under the He atmosphere. We primarily relied on detailed structural analysis of the same InCo samples provided by Bavykina *et al.*[56] to select appropriate references (Co_3O_4, CoO, and Co metal) for LCF adjustments. Figure 4 shows the Co K-edge XANES spectra of the InCo catalyst at the initial state (20 °C) after heating under He to 300 °C and then after pressurization to 50 bar at 300 °C. The evolution of the XANES spectra during temperature and pressure ramping is shown in Fig. S4 in the supplementary material. In addition, Fig. 4(b) shows the corresponding evolution of the phase amounts of different cobalt species. LCF analysis of various cobalt references reveals the presence of CoO and Co_3O_4 species predominantly at the initial stage of treatment. As the temperature rises, there is a partial reduction in cobaltite, leading to the emergence of Co metal species. The phase amount of the Co metal remains nearly constant after reaching 150 °C. After thermal treatment, the main detected species by LCF include CoO (~64%), Co metal (~25%), and Co_3O_4 (~11%).

Following the thermal treatment under He, the reaction mixture was introduced into the reactor cell at 300 °C and 50 bar, and the reaction was monitored during 24 h. Figure 5(a) shows the temporal evolution of CO_2 conversion using the high-pressure/high-temperature reaction cell. The conversion remains relatively constant at around 16% throughout the duration of the reaction. These results closely reproduce those obtained in a catalytic test conducted in a laboratory microreactor[56] (see the experimental details in Sec. S5 in the supplementary material), wherein a stable CO_2 conversion at around 13% is shown [Fig. 5(b)]. This alignment validates the performance of our high-pressure/high-temperature reaction cell for *operando* characterization.

The InCo catalyst was characterized at the final state after 24 h of reaction. The XAS spectra were collected at 300 °C and 50 bar under the reaction mixture. The structural characterization of InCo catalysts under the same conditions by Bavykina *et al.*[56] demonstrated that the catalyst surface state is modified after the reaction. Specifically, surface characterization by high-resolution XPS revealed that this modification was induced by the transformation of a part of the cobalt oxide initially present in metallic/carbides. The formation of carbides was further confirmed by elemental analyses, which showed an increase in carbon composition from 13% before the reaction to 24% after the reaction.[56] Based on these results, metallic Co, CoO, and CoInC references were selected for the LCF analyses applied to the XANES spectra after 24 h of CO_2 hydrogenation. LCF of the spectra at the final state indicates a complete disappearance of Co_3O_4 species. The evolved material comprises CoO (~41%) and Co metal (~46%) phases, alongside a residual presence of InCo carbide (~13%) species [Fig. 5(c)]. These findings align with the results obtained through ADF-STEM imaging and EELS-based elemental mapping of an identical sample after CO_2 hydrogenation, performed by Bavykina *et al.*[56] Consequently, these results demonstrate the reduction in Co_3O_4 oxide to metallic cobalt and carbide during the reaction.

A further qualitative examination of the EXAFS oscillation and Fourier transforms (FTs) at the initial state, after thermal treatment under He at 300 °C and 50 bar and after CO_2 hydrogenation reaction was carried out to have a clearer idea of the nature of the Co species present in the catalyst at different stages of the catalytic cycle. The k^2-weighted EXAFS spectra are shown in Fig. 6(a), and the corresponding pseudo-radial distribution functions of the EXAFS spectra (FT-EXAFS) of the catalyst comparing to those

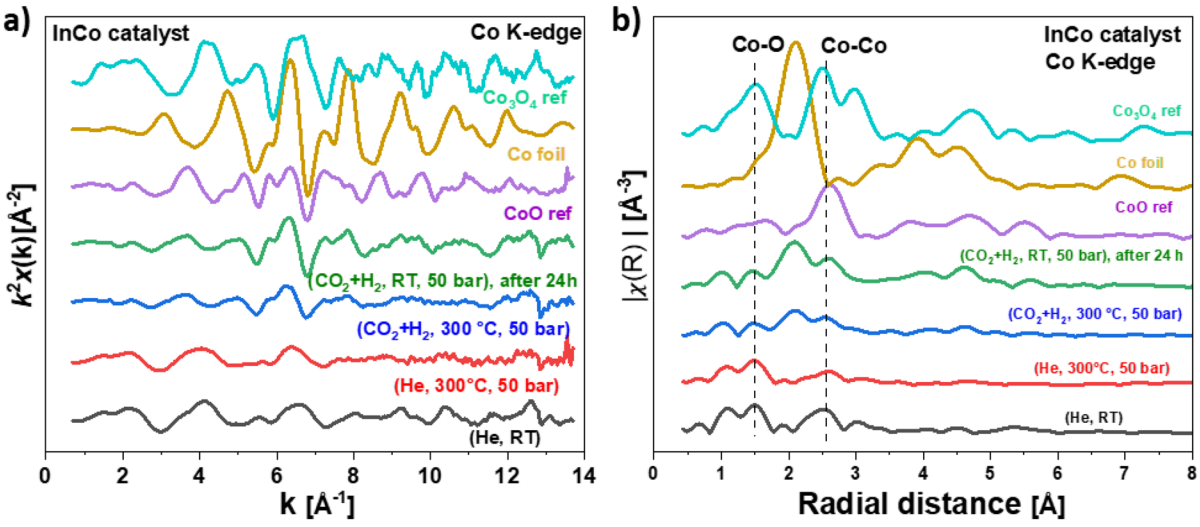

FIG. 6. (a) Co K-edge EXAFS $k^2 \cdot \chi(k)$ functions of the InCo catalyst at different cycles of the CO_2 hydrogenation reaction, compared to those of the Co foil, CoO, and Co_3O_4 reference compounds. (b) The corresponded Co K-edge *operando* FT-EXAFS spectra.

of different references (Co foil, CoO, and Co_3O_4) are showed in Fig. 6(b).

FT-EXAFS spectra of the Co foil exhibit one major feature around 2.2 Å corresponding to the Co–Co metallic bond contribution. However, the Co_3O_4 reference displayed three major signals at 1.5, 2.5, and 3 Å, identified as Co–O, octahedral Co–Co, and tetrahedral Co–Co bond contributions, respectively.[63–65] At the initial state, the cobalt in the InCo as-prepared sample predominantly exhibited a Co_3O_4 structure. This is evident from the appearance of two distinct peaks at 1.5 Å (Co–O) and 2.5 Å (octahedral Co–Co), indicative of its crystalline arrangement (the black spectra shown in Fig. 6(b). This observation aligns with the results of the LCF analysis [Fig. 5(c)], which show that the InCo catalyst in its initial state is predominantly composed of 1.5 Å Co_3O_4 species (more than 50%). Then, after thermal treatment at 300 °C and 50 bar under He, the sample retains its oxide state as indicated by the Co–O peak still present at 1.5 Å. During CO_2 hydrogenation reaction at 300 °C and 50 bar, we observe a decrease in the intensity of the peak at 1.5 Å corresponding to the Co–O bond [the blue spectra shown in Fig. 6(b)]. In parallel, a new peak emerges around 2.2 Å, corresponding to the Co–Co bond observed in the metallic cobalt foil. This transformation aligns with the LCF analyses and confirms the partial reduction of Co_3O_4 oxide to metallic cobalt during the reaction. This result may indicate that the active cobalt phase in the bimetallic InCo catalyst in the CO_2 hydrogenation reaction is present as a mixture of cobalt oxide and metallic cobalt. After the reaction (the green spectra shown in Fig. 6(b), the InCo catalyst retains the same cobalt species (mixture of oxide and metal) present during the reaction. These findings, in conjunction with the catalytic results obtained by mass spectrometry, demonstrate that our new high-pressure/temperature reactor is capable of performing *operando* characterizations of heterogeneous catalysts under operational (high temperature/pressure) conditions.

V. CONCLUSION

In summary, our research has led to the development of a high-pressure/high-temperature reactor cell dedicated for catalyst characterization using synchrotron x-ray absorption spectroscopy. The conception of the cell design enables operation at temperatures of up to 1000 °C and pressures of up to 1000 bar, depending on the gas environment. Configured for both XAS transmission and fluorescence modes, it facilitates analysis of samples containing low element concentration. In addition, the design ensures precise sample heating control, maintaining a stable and uniform temperature profile throughout the catalytic bed. Inspired by the work of Bavykina *et al.*,[56] our study highlights the practical application of the newly developed high-pressure/high-temperature reaction cell. The *operando* XAS measurements at the Co K-edge offer valuable insights into the behavior of the InCo catalyst during CO_2 hydrogenation at 300 °C and 50 bar, enhancing our understanding of its reactivity under operational conditions. On the one hand, the achieved results demonstrate the efficiency of the cell in replicating catalytic performances observed in the laboratory and, on the other hand, the potential for obtaining high-quality XAS spectra in complex conditions, providing an understanding of catalyst behavior in real-conditions.

SUPPLEMENTARY MATERIAL

The supplementary material contains more technical details regarding sample preparation within the carbon reactor, laboratory catalytic tests, and, notably, the certification of pressure tests conducted using the high-pressure/high-temperature cell.

ACKNOWLEDGMENTS

This work was supported by the French National Research Agency through the PEPR PIA4 project DIADEM "ESRF." We acknowledge SOLEIL for provision of the synchrotron radiation facilities, and we thank Dr. Emiliano Fonda and Dr. Andrea Zitolo for their assistance in using beamline SAMBA. The authors thank Dr. Anastasiya Bavykina for her contributions to the laboratory microreactor catalytic testing of CO_2 hydrogenation conducted at KAUST.

AUTHOR DECLARATIONS

Conflict of Interest

The authors have no conflicts to disclose.

Author Contributions

Abdallah Nassereddine: Conceptualization (equal); Data curation (equal); Formal analysis (equal); Writing – original draft (equal). **Alain Prat**: Methodology (equal); Writing – review & editing (equal). **Samy Ould-Chikh**: Conceptualization (equal); Data curation (equal); Methodology (equal); Visualization (equal); Writing – review & editing (equal). **Eric Lahera**: Methodology (equal). **Olivier Proux**: Conceptualization (equal); Data curation (equal); Methodology (equal); Visualization (equal); Writing – review & editing (equal). **William Delnet**: Methodology (equal). **Anael Costes**: Funding acquisition (equal). **Isabelle Maurin**: Writing – review & editing (equal). **Isabelle Kieffer**: Methodology (equal). **Sophie Min**: Methodology (equal). **Mauro Rovezzi**: Methodology (equal). **Denis Testemale**: Methodology (equal). **Jose Luis Cerrillo Olmo**: Data curation (equal). **Jorge Gascon**: Supervision (equal); Visualization (equal). **Jean-Louis Hazemann**: Methodology (equal); Supervision (equal); Validation (equal); Visualization (equal); Writing – review & editing (equal). **Antonio Aguilar Tapia**: Conceptualization (equal); Data curation (equal); Formal analysis (equal); Investigation (equal); Methodology (equal); Writing – review & editing (equal).

DATA AVAILABILITY

The data that support the findings of this study are available from the corresponding author upon reasonable request.

REFERENCES

[1] J. Wisniak, "The history of catalysis. From the beginning to Nobel prizes," Educ. Quim. **21**, 60–69 (2010).

[2] J. J. Villora-Picó, J. González-Arias, L. Pastor-Pérez, J. A. Odriozola, and T. Reina, "A review on high-pressure heterogeneous catalytic processes for gas-phase CO_2 valorization," Environ. Res. **240**, 117520 (2024).

[3] P. T. Anastas, L. B. Bartlett, M. M. Kirchhoff, and T. C. Williamson, "The role of catalysis in the design, development, and implementation of green chemistry," Catal. Today **55**, 11–22 (2000).

[4] P. T. Anastas, M. M. Kirchhoff, and T. C. Williamson, "Catalysis as a foundational pillar of green chemistry," Appl. Catal., A **221**, 3–13 (2001).

[5] Q. Liu, L. Wu, R. Jackstell, and M. Beller, "Using carbon dioxide as a building block in organic synthesis," Nat. Commun. **6**, 5933 (2015).

[6] H. Wu, J. Liu, H. Liu, and D. He, "CO_2 reforming of methane to syngas at high pressure over bi-component Ni–Co catalyst: The anti-carbon deposition and stability of catalyst," Fuel **235**, 868–877 (2019).

[7] J. Dou, Z. Sun, A. A. Opalade, N. Wang, W. Fu, and F. F. Tao, "Operando chemistry of catalyst surfaces during catalysis," Chem. Soc. Rev. **46**, 2001–2027 (2017).

[8] J. C. Bart and G. Vlaic, "Extended X-ray absorption fine structure studies in catalysis," Adv. Catal. **35**, 1–138 (1987).

[9] Y. Iwasawa, "X-ray absorption fine structure for catalysts and surfaces," Ser. Synchrotron Radiat. Tech. Appl. **2**, 428 (1996).

[10] O. Alexeev and B. C. Gates, "EXAFS characterization of supported metal-complex and metal-cluster catalysts made from organometallic precursors," Top. Catal. **10**, 273–293 (2000).

[11] A. E. Russell and R. Abigail, "X-ray absorption spectroscopy of low temperature fuel cell catalysts," Chem. Rev. **104**, 4613–463610 (2004).

[12] J. D. Grunwaldt and A. Baiker, "In situ spectroscopic investigation of heterogeneous catalysts and reaction media at high pressure," Phys. Chem. Chem. Phys. **7**, 3526–3539 (2005).

[13] S. Bordiga, E. Groppo, G. Agostini, J. A. van Bokhoven, and C. Lamberti, "Reactivity of surface species in heterogeneous catalysts probed by in situ X-ray absorption techniques," Chem. Rev. **113**, 1736–1850 (2013).

[14] X. Shi, X. Lin, R. Luo, S. Wu, L. Li, Z. J. Zhao, and J. Gong, "Dynamics of heterogeneous catalytic processes at operando conditions," JACS Au **1**, 2100–2120 (2021).

[15] N. Ichikuni, O. Kazu, and I. Yasuhiro, "X-ray absorption fine structure techniques for nano-catalytic materials," in *Advanced Characterization of Nanostructured Materials: Probing the Structure and Dynamics of Synchrotron X-Rays and Neutrons*, World Scientific Series in Nanoscience and Nanotechnology: Volume 21, edited by S. K. Sinha, M. K. Sanyal, and C. K. Loong (World Scientific, 2021), pp. 359–398.

[16] F. W. Lytle, P. S. P. Wei, R. B. Greegor, G. H. Via, and J. H. Sinfelt, "Effect of chemical environment on magnitude of x-ray absorption resonance at L_{III} edges. Studies on metallic elements, compounds, and catalysts," J. Chem. Phys. **70**, 4849–4855 (1979).

[17] S. J. A. Figueroa *et al.*, "Innovative insights in a plug flow microreactor for operando X-ray studies," J. Appl. Crystallogr. **46**, 1523–1527 (2013).

[18] J. D. Grunwaldt, M. Caravati, S. Hannemann, and A. Baiker, "X-Ray absorption spectroscopy under reaction conditions: Suitability of different reaction cells for combined catalyst characterization and time-resolved studies," Phys. Chem. Chem. Phys. **6**, 3037–3047 (2004).

[19] B. S. Clausen, G. Steffensen, B. Fabius, J. Villadsen, R. Feidenhans, and H. Topsøe, "*In situ* cell for combined XRD and on-line catalysis tests: Studies of Cu-based water gas shift and methanol catalysts," J. Catal. **132**, 524–535 (1991).

[20] G. Sankar, P. A. Wright, S. Natarajan, J. M. Thomas, G. N. Greaves, A. J. Dent, B. R. Dobson, C. A. Ramsdale, and R. H. Jones, "Combined QuEXAFS-XRD: A new technique in high-temperature materials chemistry; an illustrative in situ study of the zinc oxide-enhanced solid-state production of cordierite from a precursor zeolite," J. Phys. Chem. **97**, 9550–9554 (1993).

[21] J. D. Grunwaldt, N. V. Vegten, A. Baiker, and W. V. Beek, "Insight into the structure of Pd/ZrO_2 during the total oxidation of methane using combined in situ XRD, X-ray absorption and Raman spectroscopy," J. Phys.: Conf. Ser. **190**, 012160 (2009).

[22] W. van Beek, O. V. Safonova, G. Wiker, and H. Emerich, "SNBL, a dedicated beamline for combined *in situ* X-ray diffraction, X-ray absorption and Raman scattering experiments," Phase Transitions **84**, 726–732 (2011).

[23] B. Mutz, P. Sprenger, W. Wang, D. Wang, W. Kleist, and J. D. Grunwaldt, "Operando Raman spectroscopy on CO_2 methanation over alumina-supported Ni, Ni_3Fe and $NiRh_{0.1}$ catalysts: Role of carbon formation as possible deactivation pathway," Appl. Catal., A **556**, 160–171 (2018).

[24] M. A. Serrer, K. F. Kalz, E. Saraçi, H. Lichtenberg, and J. D. Grunwaldt, "Role of iron on the structure and stability of $Ni_{3.2}Fe/Al_2O_3$ during dynamic CO_2 methanation for P2X applications," ChemCatChem **11**, 5018–5021 (2019).

[25] B. Mutz, A. M. Gänzler, M. Nachtegaal, O. Müller, R. Frahm, W. Kleist, and J. D. Grunwaldt, "Surface oxidation of supported Ni particles and its impact on the catalytic performance during dynamically operated methanation of CO_2," Catalysts **7**, 279 (2017).

[26] A. Bansode, G. Guilera, V. Cuartero, L. Simonelli, M. Avila, and A. Urakawa, "Performance and characteristics of a high pressure, high temperature capillary cell with facile construction for operando x-ray absorption spectroscopy," Rev. Sci. Instrum. **85**, 084105 (2014).

[27] J. D. Grunwaldt, R. Wandeler, and A. Baiker, "Supercritical fluids in catalysis: Opportunities of in situ spectroscopic studies and monitoring phase behavior," Catal. Rev. **45**, 1–96 (2003).

[28] S. D. Jacques, O. Leynaud, D. Strusevich, P. Stukas, P. Barnes, G. Sankar, M. Sheehy, M. G. O'Brien, A. Iglesias-Juez, and A. M. Beale, "Recent progress in the use of in situ X-ray methods for the study of heterogeneous catalysts in packed-bed capillary reactors," Catal. Today **145**, 204–212 (2009).

[29] Y. Iwasawa, K. Asakura, and M. Tada, *XAFS Techniques for Catalysts, Nanomaterials, and Surfaces* (Springer International Publishing, Cham, 2017), pp. 275–520.

[30] S. R. Bare, N. Yang, S. D. Kelly, G. E. Mickelson, and F. S. Modica, "Design and operation of a high pressure reaction cell for in situ X-ray absorption spectroscopy," Catal. Today **126**, 18–26 (2007).

[31] B. R. Fingland, F. H. Ribeiro, and J. T. Miller, "Simultaneous measurement of X-ray absorption spectra and kinetics: A fixed-bed, plug-flow operando reactor," Catal. Lett. **131**, 1–6 (2009).

[32] V. F. Kispersky, A. J. Kropf, F. H. Ribeiro, and J. T. Miller, "Low absorption vitreous carbon reactors for operando XAS: A case study on Cu/zeolites for selective catalytic reduction of NO_x by NH_3," Phys. Chem. Chem. Phys. **14**, 2229–2238 (2012).

[33] A. Rochet, V. Moizan, C. Pichon, F. Diehl, A. Berliet, and V. Briois, "*In situ* and operando structural characterisation of a Fischer–Tropsch supported cobalt catalyst," Catal. Today **171**, 186–191 (2011).

[34] L. Pandit, M. A. Serrer, E. Saraçi, A. Boubnov, and J. D. Grunwaldt, "Versatile *in situ/operando* setup for studying catalysts by X-ray absorption spectroscopy under demanding and dynamic reaction conditions for energy storage and conversion," Chem.: Methods **2**, e202100078 (2022).

[35] K. T. Arul, H. W. Chang, H. W. Shiu, C. L. Dong, and W. F. Pong, "A review of energy materials studied by in situ/operando synchrotron x-ray spectro-microscopy," J. Phys. D: Appl. Phys. **54**, 343001 (2021).

[36] A. I. Frenkel, J. A. Rodriguez, and J. G. Chen, "Synchrotron techniques for in situ catalytic studies: Capabilities, challenges, and opportunities," ACS Catal. **2**, 2269–2280 (2012).

[37] Y. Li and Z. Wu, "A review of in situ/operando studies of heterogeneous catalytic hydrogenation of CO_2 to methanol," Catal. Today **420**, 114029 (2023).

[38] L. Fang, S. Seifert, R. E. Winans, and T. Li, "Understanding synthesis and structural variation of nanomaterials through in situ/operando XAS and SAXS," Small **18**, 2106017 (2022).

[39] A. Aguilar-Tapia, S. Ould-Chikh, E. Lahera, A. Prat, W. Delnet, O. Proux, I. Kieffer, J. M. Basset, K. Takanabe, and J. L. Hazemann, "A new high temperature reactor for operando XAS: Application for the dry reforming of methane over Ni/ZrO_2 catalyst," Rev. Sci. Instrum. **89**, 035109 (2018).

[40] B. AlSabban, L. Falivene, S. M. Kozlov, A. Aguilar-Tapia, S. Ould-Chikh, J. L. Hazemann, L. Cavallo, J. M. Basset, and K. Takanabe, "In-operando elucidation of bimetallic CoNi nanoparticles during high-temperature CH_4/CO_2 reaction," Appl. Catal., B **213**, 177–189 (2017).

[41] S. De, S. Ould-Chikh, A. Aguilar, J. L. Hazemann, A. Zitolo, A. Ramirez, S. Telalovic, and J. Gascon, "Stable Cr-MFI catalysts for the nonoxidative dehydrogenation of ethane: Catalytic performance and nature of the active sites," ACS Catal. **11**, 3988–3995 (2021).
[42] M. Wei, L. Huang, L. Li, F. Ai, J. Su, and J. Wang, "Coordinatively unsaturated PtCo flowers assembled with ultrathin nanosheets for enhanced oxygen reduction," ACS Catal. **12**, 6478–6485 (2022).
[43] A. Dokania *et al.*, "Designing a multifunctional catalyst for the direct production of gasoline-range isoparaffins from CO_2," JACS Au **1**, 1961–1974 (2021).
[44] S. De, A. Aguilar-Tapia, S. Ould-Chikh, A. Zitolo, J. L. Hazemann, G. Shterk, A. Ramirez, and J. Gascon, "Pure silica-supported transition metal catalysts for the non-oxidative dehydrogenation of ethane: Confinement effects on the stability," J. Mater. Chem. A **10**, 9445–9456 (2022).
[45] M. Çağlayan *et al.*, "Understanding W/H-ZSM-5 catalysts for the dehydroaromatization of methane," Catal. Sci. Technol. **13**, 2748–2762 (2023).
[46] G. A. Olah, A. Goeppert, and G. K. S. Prakash, "Chemical recycling of carbon dioxide to methanol and dimethyl ether: From greenhouse gas to renewable, environmentally carbon neutral fuels and synthetic hydrocarbons," J. Org. Chem. **74**, 487–498 (2009).
[47] A. Álvarez, A. Bansode, A. Urakawa, A. V. Bavykina, T. A. Wezendonk, M. Makkee, J. Gascon, and F. Kapteijn, "Challenges in the greener production of formates/formic acid, methanol, and DME by heterogeneously catalyzed CO_2 hydrogenation processes," Chem. Rev. **117**, 9804–9838 (2017).
[48] A. A. Kiss, J. J. Pragt, H. J. Vos, G. Bargeman, and M. T. De Groot, "Novel efficient process for methanol synthesis by CO_2 hydrogenation," Chem. Eng. J. **284**, 260–269 (2016).
[49] A. González-Garay, M. S. Frei, A. Al-Qahtani, C. Mondelli, G. Guillén-Gosálbez, and J. Pérez-Ramírez, "Plant-to-planet analysis of CO_2-based methanol processes," Energy Environ. Sci. **12**, 3425–3436 (2019).
[50] G. A. Olah, "Beyond oil and gas: The methanol economy," Angew. Chem., Int. Ed. **44**, 2636–2639 (2005).
[51] I. Yarulina *et al.*, "Structure–performance descriptors and the role of Lewis acidity in the methanol-to-propylene process," Nat. Chem. **10**, 804–812 (2018).
[52] A. Dutta, I. A. Karimi, and S. Farooq, "Technoeconomic perspective on natural gas liquids and methanol as potential feedstocks for producing olefins," Ind. Eng. Chem. Res. **58**, 963–972 (2018).
[53] I. Yarulina, A. D. Chowdhury, F. Meirer, B. M. Weckhuysen, and J. Gascon, "Recent trends and fundamental insights in the methanol-to-hydrocarbons process," Nat. Catal. **1**, 398–411 (2018).
[54] A. Pustovarenko *et al.*, "Metal–organic framework-derived synthesis of cobalt indium catalysts for the hydrogenation of CO_2 to methanol," ACS Catal. **10**, 5064–5076 (2020).
[55] M. Abou Hamdan, A. Nassereddine, R. Checa, M. Jahjah, C. Pinel, L. Piccolo, and N. Perret, "Supported molybdenum carbide and nitride catalysts for carbon dioxide hydrogenation," Front. Chem. **8**, 452 (2020).
[56] A. Bavykina *et al.*, "Turning a methanation Co catalyst into an In–Co methanol producer," ACS Catal. **9**, 6910–6918 (2019).
[57] D. Testemale, R. Argoud, O. Geaymond, and J. L. Hazemann, "High pressure/high temperature cell for x-ray absorption and scattering techniques," Rev. Sci. Instrum. **76**, 043905 (2005).
[58] See http://www.htw-gmbh.de/index.php5?lang=en&nav0=0 for Hochtempe ratur–Werkstoffe (GmbH).
[59] K. Tamura, M. Inui, and S. Hosokawa, "XAFS measurements at high temperatures and pressures," Rev. Sci. Instrum. **66**, 1382–1384 (1995).
[60] S. Belin, V. Briois, A. Traverse, M. Idir, T. Moreno, and M. Ribbens, "SAMBA a new beamline at SOLEIL for x-ray absorption spectroscopy in the 440 keV energy range," Phys. Scr. **2005**, 980.
[61] B. Ravel and M. A. Newville, "*ATHENA*, *ARTEMIS*, *HEPHAESTUS*: Data analysis for X-ray absorption spectroscopy using *IFEFFIT*," J. Synchrotron Radiat. **12**, 537–541 (2005).
[62] S. M. Webb, "Fingerprinting: Principal component analysis and linear combination fitting," Int. Tables Crystallogr. **26**, 483 (2023).
[63] J. Huang, H. Sheng, R. D. Ross, J. Han, X. Wang, B. Song, and S. Jin, "Modifying redox properties and local bonding of Co_3O_4 by CeO_2 enhances oxygen evolution catalysis in acid," Nat. Commun. **12**, 3036 (2021).
[64] Y. Zhu, J. Wang, T. Koketsu, M. Kroschel, J. M. Chen, S. Y. Hsu, G. Henkelman, Z. Hu, P. Strasser, and J. Ma, "Iridium single atoms incorporated in Co_3O_4 efficiently catalyze the oxygen evolution in acidic conditions," Nat. Commun. **13**, 7754 (2022).
[65] F. Yu, T. Huo, Q. Deng, G. Wang, Y. Xia, H. Li, and W. Hou, "Single-atom cobalt-hydroxyl modification of polymeric carbon nitride for highly enhanced photocatalytic water oxidation: Ball milling increased single atom loading," Chem. Sci. **13**, 754–762 (2022).